Neoplasia • Vol. 8, No. 10, October 2006, pp. 826–832 826

www.neoplasia.com

TMPRSS2–ERG Gene Fusion Causing *ERG* Overexpression Precedes Chromosome Copy Number Changes in Prostate Carcinomas and Paired HGPIN Lesions[1]

Nuno Cerveira, Franclim R. Ribeiro*, Ana Peixoto*, Vera Costa*, Rui Henrique†,‡, Carmen Jerónimo*,‡,§ and Manuel R. Teixeira*,‡*

*Department of Genetics, Portuguese Oncology Institute, Porto, Portugal; †Department of Pathology, Portuguese Oncology Institute, Porto, Portugal; ‡Department of Pathology and Molecular Immunology, Institute of Biomedical Sciences, University of Porto, Porto, Portugal; §Fernando Pessoa University School of Health Sciences, Porto, Portugal

Abstract

***TMPRSS2–ETS* gene fusions have been found recurrently in prostate carcinomas, but not in the presumed precursor lesion, high-grade prostatic intraepithelial neoplasia (HGPIN). However, HGPIN lesions may share chromosomal changes with prostate cancer. To determine the relative order of genetic events in prostate carcinogenesis, we have analyzed 34 prostate carcinomas, 19 paired HGPIN lesions, 14 benign prostate hyperplasias, and 11 morphologically normal prostatic tissues for *TMPRSS2–ERG* and *TMPRSS2–ETV1* rearrangements and genomic imbalances. *TMPRSS2* exon 1 was fused in-frame with *ERG* exon 4 in 17 of 34 (50%) prostate carcinomas and in 4 of 19 (21%) HGPIN lesions, but in none of controls. The findings were further validated by sequencing analysis and by the real-time polymerase chain reaction quantification of *TMPRSS2–ERG* fusion transcript and the *ERG* exons 5/6:exons 1/2 expression ratio. Chromosome copy number changes were detected by comparative genomic hybridization in 42% of clinically confined carcinomas and in none of the 16 HGPIN lesions analyzed. We demonstrate for the first time that the *TMPRSS2–ERG* fusion gene can be detected in a proportion of HGPIN lesions and that this molecular rearrangement is an early event that may precede chromosome-level alterations in prostate carcinogenesis.**

Neoplasia (2006) **8,** 826–832

Keywords: *TMPRSS2–ETS* fusion oncogenes, prostate cancer, high-grade prostatic intraepithelial neoplasia, chromosomal changes, *ERG*.

Introduction

A central aim in cancer research is to identify genes that play a causal role in cancer development. Many such genes have been identified through analyses of recurrent chromosomal rearrangements that are characteristic of leukemias, lymphomas, and sarcomas, typically resulting in the formation of oncogenic fusion genes [1]. This type of specific genetic change has only rarely been detected in common solid cancers [2], although that can be related to the smaller number of cases analyzed [3,4]. Recently, taking advantage of a bioinformatic approach termed Cancer Outlier Profile Analysis, the fusion genes *TMPRSS2–ERG* and *TMPRSS2–ETV1* have been detected in a high proportion of prostate carcinomas selected for demonstrating an overexpression of the erythroblast transformation specific (ETS) transcription factor *ERG* or *ETV1* [5]. Later, a rare third fusion gene, involving the *TMPRSS2* locus and another ETS family gene *ETV4*, was identified [6].

The fusion partner common to the three rearrangements is *TMPRSS2*, an androgen-regulated member of the type II transmembrane serine protease family that maps to 21q22.3. TMPRSS2 protein is preferentially expressed in normal prostate tissues and is overexpressed in the neoplastic prostatic epithelium [7–10]. Its expression seems to be regulated by androgen-responsive elements (AREs) in a promoter [10,11], and it has been shown that androgen stimulation can induce the overexpression of *ERG* in a *TMPRSS2–ERG*–positive cell line [5]. These results suggest that deregulation of ETS transcription factor protein activity through AREs mapped 5′ of *TMPRSS2* may underlie prostate cancer development, affecting biologic processes such as cell proliferation, differentiation, development, transformation, and apoptosis [5,12].

Although *TMPRSS2–ETS* gene fusions seem to be recurrent in prostate carcinomas, this genetic abnormality has not been reported in the presumed precursor lesion, high-grade prostatic intraepithelial neoplasia (HGPIN) [5]. However, fluorescent *in situ* hybridization (FISH) and comparative

Abbreviations: HGPIN, high-grade prostatic intraepithelial neoplasia; PCa, prostate adenocarcinomas; ETS, erythroblast transformation specific; CGH, comparative genomic hybridization; RT-PCR, reverse transcriptase–polymerase chain reaction

Address all correspondence to: Manuel R. Teixeira, Department of Genetics, Portuguese Oncology Institute, Rua Dr. António Bernardino de Almeida, Porto 4200-072, Portugal.
E-mail: mteixeir@ipoporto.min-saude.pt

[1]This research was supported by research grant POCTI/SAU-OBS/58357/2004 from the Fundação para a Ciência e a Tecnologia.

Received 31 May 2006; Revised 13 July 2006; Accepted 17 July 2006.

DOI 10.1593/neo.06427

genomic hybridization (CGH) data have shown that HGPIN lesions may share genetic features with prostate cancer (e.g., 8p deletion) [13,14]. Therefore, the time of occurrence and the relative order of events in *ETS* gene fusions and chromosome imbalances are not known in prostate carcinogenesis. To address this issue, we have analyzed 34 samples of clinically localized prostate adenocarcinomas (PCa) and 19 paired HGPIN lesions for chromosome copy number changes and *TMPRSS2–ERG* and *TMPRSS2–ETV1* rearrangements.

Materials and Methods

Patient Data

Primary tumors from 34 patients with clinically localized PCa [stage II ($T_{1c}N_0M_0$ or $T_2N_0M_0$), according to the TNM staging system] who were consecutively diagnosed and primarily treated with radical prostatectomy at the Portuguese Oncology Institute (Porto, Portugal) were prospectively collected. In 19 radical prostatectomy specimens with PCa, HGPIN lesions were identified and collected for further analysis. For control purposes, non-neoplastic prostate tissue samples were obtained from 14 randomly selected patients with benign prostate hyperplasia (BPH) who underwent transurethral resection of the prostate and from the peripheral zone of 11 prostates that did not harbor prostate cancer, which were collected from cystoprostatectomy (NPT) specimens of bladder cancer patients.

Sample Collection, RNA Extraction, and cDNA Synthesis

All tissue specimens were frozen immediately after surgery and stored at −80°C for further analysis. Five-micron–thick sections were cut and stained for the identification of areas of PCa (i.e., index or dominant tumor), HGPIN, BPH, and morphologically normal tissues. Then, the tissue block was trimmed to maximize the yield of target cells (> 70% of target cells). Subsequently, an average of fifty 12-μm–thick sections were cut, and every fifth section was stained to ensure a uniform percentage of target cells and to exclude contamination from neoplastic cells in normal and BPH tissue samples. Total cellular RNA was extracted from 250 mg of (normal and tumor) tissues using the FastRNA Kit Green (Qbiogene, Carlsbad, CA) for 90 seconds, with a speed rating of 6.0 in a FastPrep FP120 Instrument (Qbiogene). For cDNA synthesis, 1 to 5 μg of RNA was subjected to reverse transcription with random hexamers using the Superscript III First-Strand Synthesis System for reverse transcriptase–polymerase chain reaction (RT-PCR) (Invitrogen, Carlsbad, CA), according to the manufacturer's instructions. Final cDNA was diluted with 30 μl of H_2O.

RT-PCR Analysis

RT-PCR for the detection of *TMPRSS2–ERG* and *TMPRSS2–ETV1* chimeric transcripts was previously described [5]. In brief, PCR was performed in a 50-μl reaction containing 2 μl of synthesized cDNA, 5 μl of 10× GeneAmp PCR Buffer II (100 mM Tris–HCl, pH 8.3, 500 mM KCl) (Applied Biosystems, Foster City, CA), 5 μl of 25 mM $MgCl_2$, 0,4 μl of dNTP mix (25 mM of each dNTP) (Applied Biosystems), 0.4 μM of each primer (Metabion, Martinsried, Deutschland), and 1 U of AmpliTaq Gold DNA Polymerase (Applied Biosystems). Reaction tubes were kept on ice at all times to prevent nonspecific amplification. Reaction tubes were incubated for 10 minutes at 95°C, followed by 35 cycles of 1 minute at 95°C, 1 minute at 63°C, and 1 minute at 72°C, followed by a final elongation of 10 minutes at 72°C on a GeneAmp PCR System 9700 (Applied Biosystems). Amplified products were analyzed on a 2% agarose gel (SeaKem LE Agarose, Rockland, MA), and the results were visualized with an image analyzer ImageMaster VDS (Amersham Biosciences, Little Chalfont, UK).

Sequence Analysis

Sequence analysis was directly performed on amplified RT-PCR products with the use of BigDye Terminator Cycle Sequencing Chemistry (Applied Biosystems) on an automated sequencer ABI Prism 310 Genetic Analyzer (Applied Biosystems), according to the manufacturer's instructions.

Real-Time PCR Analysis

Primers and probes for *TMPRSS2–ERG*, *TMPRSS2*, *ERG*, and *ETV1* were designed with Primer Express 2.0 (Applied Biosystems) and purchased from Metabion (Table 1). Primers and probes for the β-glucuronidase (*GUSB*) gene, used as endogenous control, were purchased as a predeveloped assay reagent from Applied Biosystems. To determine the relative expression levels of the target gene in each sample, the relative amount of the target gene was calibrated to the relative amount of the internal reference gene and was expressed in terms of target/reference ratios that were then multiplied by 100 for easier tabulation (target gene/*GUSB* × 100). PCR was performed in a 25-μl reaction containing 5 μl of synthesized cDNA, 12.5 μl of *TaqMan* universal PCR master mix, 0.3 μM of each primer, and 0.2 μM of each probe. PCR was performed in separate wells for each primer/probe set, and each sample was run in triplicate. PCR parameters were as follows: 50°C for 2 minutes, 95°C for 10 minutes, followed by 50 cycles at 95°C for 15 seconds and 60°C for 1 minute. Each plate included multiple nontemplate controls and serial dilutions of a positive control for constructing the standard curve.

CGH Analysis

CGH analysis followed the procedure of Kallioniemi et al. [15], with modifications, as previously described [16]. Briefly, test and reference DNA were extracted using standard methods and labeled in nick translation reactions using Spectrum Green and Spectrum Red conjugated nucleotides (Vysis, Downers Grove, IL), after which probe lengths between 300 and 2000 bp were obtained. Labeled sample and reference DNA (1 μg each) were mixed with 30 μg of unlabeled *Cot*1 DNA (Life Technologies, Rockville, MD), ethanol-precipitated, dried, and dissolved in hybridization buffer (Vysis). Probe mixture was denatured and hybridized to commercially available normal metaphase slides (Vysis)

Table 1. Oligonucleotide Primers and Probes (5′FAM and 3′TAMRA) Used in This Study.

Gene	Exon	Position	Primer/Probe*	Sequence 5′–3′
ERG	1	3–22	ERG1-S	CCCGAGGGACATGAGAGAAG
ERG	2	50–69	ERG2-AS	TTTCCTCGGGTCTCCAAAGA
ERG	1–2	26–48	ERG12-PR	AGCGGCGCTCAGGTTATTCCAGG
ERG	5	564–583	ERG5-S	CACGAACGAGCGCAGAGTTA
ERG	6	611–630	ERG6-AS	CTGCCGCACATGGTCTGTAC
ERG	5–6	585–609	ERG56-PR	CGTGCCAGCAGATCCTACGCTATGG
TMPRSS2	1	−4–17	TMPRSS2/ERG-S	TAGGCGCGAGCTAAGCAGGAG
ERG	4	252–276	TMPRSS2/ERG-AS	GTAGGCACACTCAAACAACGACTGG
TMPRSS2–ERG	–	–	TMPRSS2/ERG-PR	AGCGCGGCAGGAAGCCTTATCAGTT

The GenBank accession numbers for *TMPRSS2* and *ERG* are NM_005656.2 and NM_004449.3, respectively.
*S = sense; AS = antisense; PR = probe.

for 2 to 3 days at 37°C in a moist chamber. After washing off excess probe, samples were counterstained with DAPI in an antifade solution (Vector Laboratories, Burlingame, CA). Image analysis was performed with CytoVision System version 3.0 (Applied Imaging, Santa Clara, CA). Data from 10 cells were combined to generate average ratio profiles with 99% confidence intervals (CIs) for each sample. A standard reference interval, generated with data from 10 normal *versus* normal hybridizations (totaling 110 cells), was automatically scaled onto each sample, and aberrations were scored whenever the case profile and the standard reference profile at 99% CI did not overlap [17]. The description of CGH copy number changes followed the guidelines suggested in ISCN [18].

Results

Frequency of TMPRSS2–ERG and TMPRSS2–ETV1 Fusion Transcripts

To estimate the frequency of *TMPRSS2–ERG* and *TMPRSS2–ETV1* chimeric transcripts, we have screened a consecutive series of 34 patients with clinically localized PCa and 19 paired HGPIN. Type A *TMPRSS2–ERG* transcript could be detected in 17 of 34 (50%) prostate carcinomas and in 4 of 19 (21%) HGPIN lesions, but in none of controls (Figure 1*A*). When we consider all patient samples regardless of lesion type (i.e., PCa or HGPIN), this frequency rises to 56% (19 of 34) because, in two negative PCa cases, the corresponding HGPIN was positive (Table 2). No type B *TMPRSS2–ERG* or *TMPRSS2–ETV1* fusion transcript was detected in any of the samples analyzed. The sequencing of amplification products, followed by BLAST search, confirmed that *TMPRSS2* exon 1 was fused in-frame with *ERG2* exon 4 (Figure 1*B*).

TMPRSS2–ERG Fusion Transcript Quantification

To validate the findings regarding *TMPRSS2–ERG*, we designed a specific primer pair and probe for the type A *TMPRSS2–ERG* transcript. All RT-PCR–positive cases were quantified and, as additional negative controls, some *TMPRSS2–ERG*–negative cases were also analyzed. Only the previously identified RT-PCR–positive cases (PCa and HGPIN) showed amplification by real-time PCR, with *TMPRSS2–ERG* normalized values ranging from 1.55 to 530.63 in PCa and from 1.02 to 17.19 in HGPIN (Table 2). All *TMPRSS2–ERG*–negative cases analyzed showed no amplification by real-time PCR.

Relationship between TMPRSS2–ERG Fusion and ERG Overexpression

To evaluate the relationship between *TMPRSS2–ERG* detection and *ERG* expression in our series, we designed specific primer pairs and probes for *ERG* exons 1 and 2 and for *ERG* exons 5 and 6. Quantitative RT-PCR revealed that the *ERG* exons 5/6:exons 1/2 ratio was higher than 2.5 in all *TMPRSS2–ERG*–positive (but in none of negative) prostate carcinomas (Table 2). The relationship between the presence of *TMPRSS2–ERG* fusion and *ERG* overexpression was less constant in HGPIN lesions because only one of four positive cases for the *TMPRSS2–ERG* fusion showed an *ERG* exons 5/6:exons 1/2 ratio above 2.5. Regarding the control group, none of 11 NPT samples showed an *ERG* exons 5/6:exons 1/2 ratio above 2.5, but in one case of BPH (BPH 84), the *ERG* exons 5/6:exons 1/2 ratio was clearly above 2.5 (Table 2).

CGH Findings

Sixteen of 19 HGPIN lesions yielded enough DNA and were analyzed in the present study. Genomic data on 34 PCa and 14 BPH samples were previously published [14]. Chromosome copy number changes were detected in 42% of PCa samples (Table 2), with the most frequent alteration corresponding to 8p loss (10 of 13 samples with copy number changes). Of the 17 *TMPRSS2–ERG*–positive carcinomas, eight were shown to harbor genomic imbalances. All HGPIN lesions presented a balanced chromosome constitution. No statistically significant correlation could be established between specific genetic alterations and the presence of the *TMPRSS2–ERG* fusion transcript, but all three PCa with 8q gain did not harbor the fusion gene.

Discussion

We have confirmed that a high proportion of prostate carcinomas presents the *TMPRSS2–ERG* rearrangement. In our consecutive series of clinically localized PCa, this genetic anomaly was detected in 50% of cases, making it the most

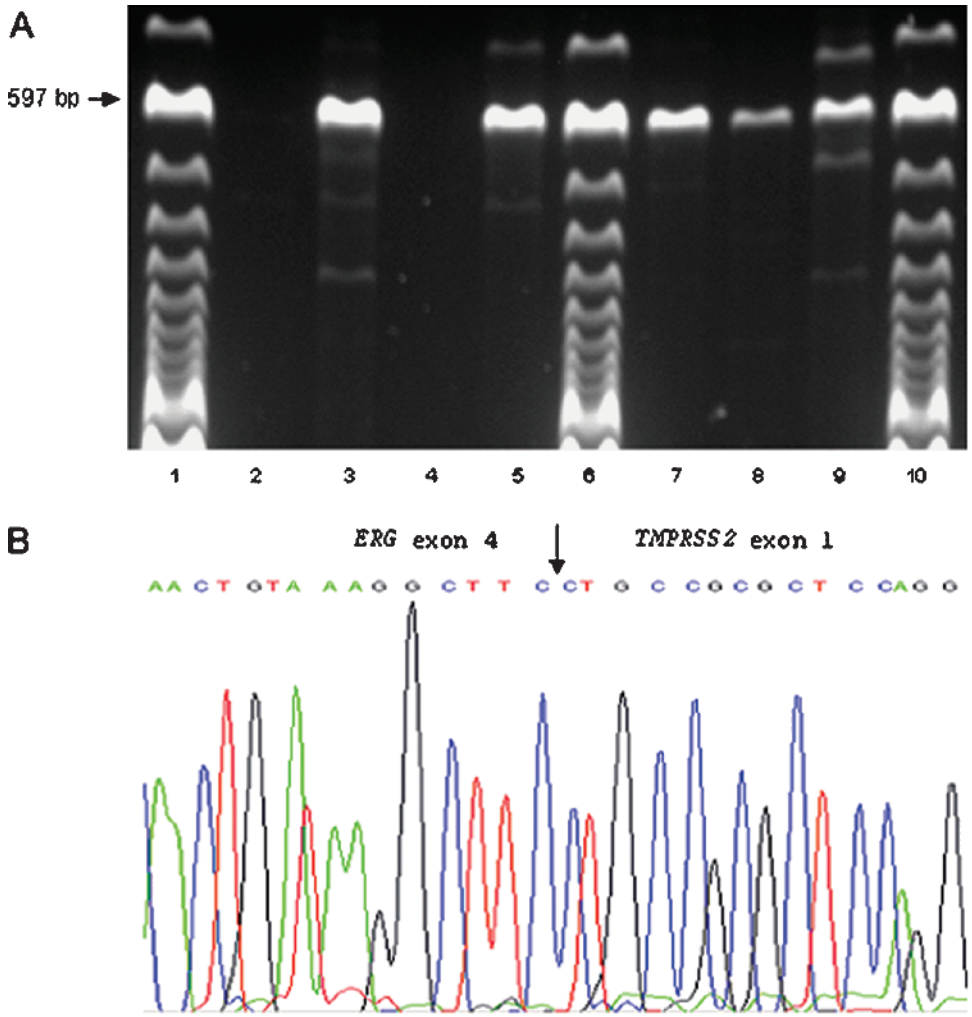

Figure 1. *Detection and analysis of type A TMPRSS2–ERG fusion transcript in prostate carcinoma and HGPIN samples. (A) RT-PCR analysis with a sense primer located in TMPRSS2 exon 1 and an antisense primer located in ERG exon 6 in PCa (PCa 55, PCa 114, PCa 134, and PCa 152 in lanes 2–5, respectively) and HGPIN (HGPIN 60, HGPIN 83, and HGPIN 42 in lanes 7–9, respectively) samples. The expected size of the type A TMPRSS2–ERG fusion transcript is indicated. Lanes 1, 6, and 10 = 100-bp molecular marker. (B) Partial sequence of the junction of type A TMPRSS2–ERG chimeric mRNA showing the nucleotide sequence of the fusion transcript. The arrow shows in-frame fusion between TMPRSS2 exon 1 and ERG exon 4.*

frequent fusion gene in human carcinomas. This finding was confirmed by quantitative real-time RT-PCR targeting the fusion gene. Furthermore, the *ERG* exons 5/6:exons 1/2 ratio was higher than 2.5 in all *TMPRSS2–ERG*–positive (but in none of negative) prostate carcinomas. Our results are in agreement with Tomlins et al. [5] who, using FISH analysis, reported the presence of *ERG* rearrangement in 55% (16 of 29) of a series of 29 prostate carcinomas selected independently of any knowledge of *ERG* or *ETV1* expression [5]. However, Soller et al. [19] reported a *TMPRSS2–ERG* fusion frequency of 79%. This discrepancy can be due to the lower number of cases (n = 18) studied by Soller et al. [19] and/or to their use of nested PCR. Indeed, when we used nested PCR in our samples, the frequency of the *TMPRSS2–ERG* transcript rose to 62%, but, additionally, three control samples (one HBP and two CP) also showed a clear positive signal (data not shown). False-positive results with highly sensitive PCR techniques for the detection of fusion transcripts are relatively rare, but are a major concern in patients with hematologic malignancies [20,21]. These can be due to contamination from previous positive cases or to the presence of very rare normal cells with abnormal molecular rearrangements characteristic of specific types of hematologic malignancies (e.g., *BCR–ABL* gene fusion in chronic myeloid leukemia and *BCL2* gene rearrangement in follicular lymphoma) [20,21]. As a consequence, one should be aware of the potential risks of using nested PCR in diagnostic samples, despite scrupulous precautions taken to minimize contamination. Conversely, *TMPRSS2–ETV1* fusion was not detected in any of our cases. This is in agreement with previous reported frequencies of 3% (1 of 32) and 0% (0 of 18) [5,18], suggesting that this molecular rearrangement, as with *TMPRSS2–ETV4* fusion [6], is not a frequent event in prostate cancer.

To the best of our knowledge, this is the first study to report on the presence of *TMPRSS2–ERG* fusion in HGPIN lesions (21% of cases in our series). The detection of the *TMPRSS2–ERG* fusion gene in HGPIN is not unexpected

Table 2. Qualitative RT-PCR (Column 2), Quantitative RT-PCR (Columns 3 and 4), and CGH (Column 5) Findings of a Consecutive Series of PCa, Paired HGPIN, BPH, and NPT Samples.

Sample ID	*TMPRSS2–ERG* RT-PCR	*TMPRSS2–ERG* Real-Time PCR	*ERG* Exons 5/6:Exons 1/2 Real-Time PCR	CGH Findings (Standard Reference Interval [SRI] 99% CI)
PCa 32	Positive, type A	19.42	4.77	Rev ish dim(8p12pter)
HGPIN 32	–	0.00	0.44	No changes
PCa 40	Positive, type A	530.63	52.45	No changes
HGPIN 40	–	0.00	1.39	No changes
PCa 42	–	ND	1.25	No changes
HGPIN 42	Positive, type A	1.02	0.79	No changes
PCa 45	Positive, type A	8.01	2.87	Rev ish dim(8p12p22)
HGPIN 45	–	ND	0.37	ND
PCa 46	–	ND	1.97	ND
HGPIN 46	–	ND	0.41	No changes
PCa 55	–	ND	2.29	Rev ish enh(3q23q26,7p13p21,7q21q32,8q21q24), dim(16q22qter)
HGPIN 55	–	0.00	4.23	No changes
PCa 56	–	ND	2.08	No changes
PCa 58	–	ND	2.38	Rev ish enh(8q21q24), dim(8p22)
HGPIN 58	Positive, type A	1.73	17.47	No changes
PCa 60	Positive, type A	37.56	4.69	No changes
HGPIN 60	Positive, type A	17.19	2.48	No changes
PCa 67	Positive, type A	120.91	111.61	Rev ish dim(8p21pter)
PCa 72	–	ND	0.44	Rev ish enh(5p14pter,5q11q23,5q32q33)
PCa 76	–	ND	1.72	Rev ish enh(8q), dim(2q23q24,8p12p23,10p11p12,10q22q25)
PCa 78	–	ND	1.73	ND
HGPIN 78	–	ND	1.85	No changes
PCa 81	Positive, type A	112.83	10.41	No changes
PCa 83	Positive, type A	24.79	13.84	No changes
HGPIN 83	Positive, type A	1.87	1.01	ND
PCa 84	–	0.00	1.34	No changes
HGPIN 84	–	ND	1.08	No changes
PCa 87	–	ND	1.35	No changes
HGPIN 87	–	ND	0.76	No changes
PCa 89	Positive, type A	149.02	7.47	No changes
PCa 101	Positive, type A	19.43	6.44	Rev ish enh(18p11), dim(8p22pter,13q14q22)
PCa 114	Positive, type A	493.30	47.07	Rev ish dim(16q22qter)
PCa 115	–	ND	2.17	No changes
HGPIN 115	–	0.00	2.98	No changes
PCa 131	–	ND	1.45	No changes
PCa 134	–	0.00	1.18	No changes
PCa 138	Positive, type A	13.58	31.49	ND
HGPIN 138	–	0.00	0.29	No changes
PCa 139	Positive, type A	62.40	59.25	Rev ish dim(8p22pter,17p13)
PCa 140	Positive, type A	11.62	5.84	No changes
PCa 145	Positive, type A	1.55	4.70	No changes
HGPIN 145	–	0.00	1.68	No changes
PCa 147	–	ND	2.24	No changes
HGPIN 147	–	ND	0.57	No changes
PCa 150	–	ND	0.53	No changes
HGPIN 150	–	ND	1.03	No changes
PCa 151	–	0.00	0.29	No changes
PCa 152	Positive, type A	206.05	9.62	No changes
PCa 156	–	ND	1.69	Rev ish dim(6q15q21,8p21p23,13q21q31)
HGPIN 156	–	0.00	0.82	ND
PCa 164	Positive, type A	57.74	6.34	Rev ish dim(8p12p22,10q22qter,13q14q21,16q23q24)
HGPIN 164	–	0.00	0.42	ND
PCa 172	Positive, type A	155.73	6.94	Rev ish dim(8p12p22,17p12pter)
NPT 1	–	ND	0.84	ND
NPT 3	–	0.00	2.08	ND
NPT 5	–	ND	0.44	ND
NPT 6	–	ND	0.45	ND
NPT 7	–	0.00	1.96	ND
NPT 8	–	ND	0.23	ND
NPT 10	–	ND	0.07	ND
NPT 11	–	ND	0.47	ND
NPT 12	–	0.00	0.19	ND
NPT 13	–	0.00	0.37	ND
NPT 14	–	0.00	0.10	ND
BPH 7	–	ND	0.70	No changes
BPH 17	–	ND	0.32	No changes
BPH 36	–	ND	0.12	No changes
BPH 55	–	ND	0.38	No changes
BPH 68	–	ND	0.06	No changes
BPH 71	–	ND	0.08	No changes
BPH 76	–	ND	0.35	No changes

Table 2. (*continued*)

Sample ID	*TMPRSS2–ERG* RT-PCR	*TMPRSS2–ERG* Real-Time PCR	*ERG* Exons 5/6:Exons 1/2 Real-Time PCR	CGH Findings (SRI 99% CI)
BPH 79	–	0.00	2.05	No changes
BPH 84	–	0.00	24.68	No changes
BPH 89	–	0.00	0.40	No changes
BPH 91	–	ND	0.32	No changes
BPH 92	–	ND	0.16	No changes
BPH 96	–	ND	0.28	No changes

ND, not done.

because this lesion is considered to be a precursor of, at least, some prostate carcinomas [22]. Indeed, histologic data seem to support this hypothesis: HGPIN consists of architecturally benign prostatic acini lined by cells that seem to be malignant (Figure 2), and prostate carcinomas may have zones of HGPIN from which glands of carcinoma seem to stem [22–24]. In addition, prostates with carcinoma have more of these foci than do those without carcinoma; prostate glands with extensive HGPIN also have more multifocal carcinomas; and HGPIN lesions preferentially develop in the peripheral zone of the prostate, which is the site of origin for most adenocarcinomas [22,25]. Interestingly, in two patients (cases 42 and 58), the fusion transcript was detected in the HGPIN lesion, but not in the PCa present in the same gland. This observation supports the hypothesis that prostate carcinogenesis may be a multicentric process, in which at least two independent pathogenetic pathways may coexist in the same prostate, leading to independent neoplasias with or without the involvement of the ETS pathway.

As opposed to prostate carcinomas with *TMPRSS2–ERG* fusion, where a clear association between *TMPRSS2–ERG* positivity and *ERG* overexpression was observed, this relationship was less constant in HGPIN lesions, with only one of four positive cases for the *TMPRSS2–ERG* fusion showing an *ERG* exons 5/6:exons 1/2 ratio above 2.5. These findings are compatible with the hypothesis that HGPIN lesions may initially be polyclonal proliferations, with the cells with *TMPRSS2–ERG* fusion being diluted in a pool of cells not harboring this alteration. Presumably, the HGPIN lesion may eventually be dominated by the clone with the *TMPRSS2–ERG* fusion as a result of clonal expansion, as shown by the detection of *ERG* overexpression in a subset of HGPIN lesions.

Although no correlation could be established between specific copy number changes detected by CGH and the presence of the *TMPRSS2–ERG* fusion transcript or *ERG* overexpression, several interesting conclusions can be drawn from our results. When we consider the group of PCa and HGPIN samples with *TMPRSS2–ERG* fusion, only eight of PCa cases and none of HGPIN samples showed copy number changes by CGH, indicating that the *TMPRSS2–ERG* fusion is an early pathogenetic event in prostate carcinogenesis that precedes the acquisition of chromosome imbalances. Because none of the *TMPRSS2–ERG*–positive cases showed a gain of 8q, a genomic imbalance recently identified as an independent predictor of poor survival [16], it is possible that the *TMPRSS2–ERG* gene fusion could represent a class of clinically less aggressive prostate carcinomas, but this needs to be addressed in a larger series.

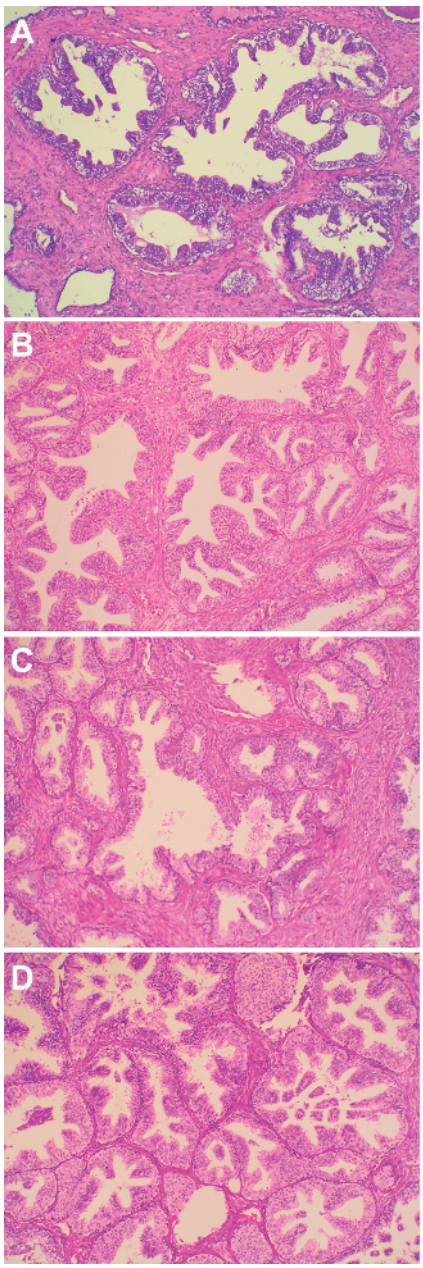

Figure 2. *Representative images of four HGPIN lesions harboring the TMPRSS2–ERG fusion gene. (A) HGPIN 42. (B) HGPIN 58. (C) HGPIN 60. (D) HGPIN 83 (hematoxylin–eosin stain; original magnification, ×25).*

In summary, we confirm that fusion of the ETS transcription factor *ERG* with the *TMPRSS2* gene is a frequent event in prostate cancer. Furthermore, we demonstrate for the first time that *TMPRSS2–ERG* fusion can already be detected in a proportion of HGPIN lesions and that this molecular rearrangement is an early event that may precede chromosome-level alterations in prostate carcinogenesis.

References

[1] Rowley JD (2001). Chromosome translocations: dangerous liaisons revisited. *Nat Rev Cancer* **1,** 245–250.

[2] Mitelman F (2000). Recurrent chromosome aberrations in cancer. *Mutat Res* **462,** 247–253.

[3] Mitelman F, Johansson B, and Mertens F (2004). Fusion genes and rearranged genes as a linear function of chromosome aberrations in cancer. *Nat Genet* **36,** 331–334.

[4] Mitelman F, Mertens F, and Johansson B (2005). Prevalence estimates of recurrent balanced cytogenetic aberrations and gene fusions in unselected patients with neoplastic disorders. *Genes Chromosomes Cancer* **43,** 350–366.

[5] Tomlins SA, Rhodes DR, Perner S, Dhanasekaran SM, Mehra R, Sun XW, Varambally S, Cao X, Tchinda J, Kuefer R, et al. (2005). Recurrent fusion of *TMPRSS2* and *ETS* transcription factor genes in prostate cancer. *Science* **310,** 644–648.

[6] Tomlins SA, Mehra R, Rhodes DR, Smith LR, Roulston D, Helgeson BE, Cao X, Wei JT, Rubin MA, Shah RB, et al. (2006). *TMPRSS2:ETV4* gene fusions define a third molecular subtype of prostate cancer. *Cancer Res* **66,** 3396–3400.

[7] Hooper JD, Clements JA, Quigley JP, and Antalis TM (2001). Type II transmembrane serine proteases. Insights into an emerging class of cell surface proteolytic enzymes. *J Biol Chem* **276,** 857–860.

[8] Netzel-Arnett S, Hooper JD, Szabo R, Madison EL, Quigley JP, Bugge TH, and Antalis TM (2003). Membrane anchored serine proteases: a rapidly expanding group of cell surface proteolytic enzymes with potential roles in cancer. *Cancer Metastasis Rev* **22,** 237–258.

[9] Vaarala MH, Porvari K, Kyllonen A, Lukkarinen O, and Vihko P (2001). The *TMPRSS2* gene encoding transmembrane serine protease is overexpressed in a majority of prostate cancer patients: detection of mutated *TMPRSS2* form in a case of aggressive disease. *Int J Cancer* **94,** 705–710.

[10] Afar DE, Vivanco I, Hubert RS, Kuo J, Chen E, Saffran DC, Raitano AB, and Jakobovits A (2001). Catalytic cleavage of the androgen-regulated TMPRSS2 protease results in its secretion by prostate and prostate cancer epithelia. *Cancer Res* **61,** 1686–1692.

[11] Lin B, Ferguson C, White JT, Wang S, Vessella R, True LD, Hood L, and Nelson PS (1999). Prostate-localized and androgen-regulated expression of the membrane-bound serine protease TMPRSS2. *Cancer Res* **59,** 4180–4184.

[12] Seth A and Watson DK (2005). ETS transcription factors and their emerging roles in human cancer. *Eur J Cancer* **41,** 2462–2478.

[13] Foster CS, Bostwick DG, Bonkhoff H, Damber JE, van der Kwast T, Montironi R, and Sakr WA (2000). Cellular and molecular pathology of prostate cancer precursors. *Scand J Urol Nephrol* **205,** 19–43.

[14] Ribeiro FR, Diep CB, Jeronimo C, Henrique R, Lopes C, Eknaes M, Lingjaerde OC, Lothe RA, and Teixeira MR (2006). Statistical dissection of genetic pathways involved in prostate carcinogenesis. *Genes Chromosomes Cancer* **45,** 154–163.

[15] Kallioniemi OP, Kallioniemi A, Piper J, Isola J, Waldman FM, Gray JW, and Pinkel D (1994). Optimizing comparative genomic hybridization for analysis of DNA sequence copy number changes in solid tumors. *Genes Chromosomes Cancer* **10,** 231–243.

[16] Ribeiro FR, Jerónimo C, Henrique R, Fonseca D, Oliveira J, Lothe RA, and Teixeira MR (2006). 8q gain is an independent predictor of poor survival in diagnostic needle biopsies from prostate cancer suspects. *Clin Cancer Res* **12,** 3961–3970.

[17] Kirchhoff M, Gerdes T, Rose H, Maahr J, Ottesen AM, and Lundsteen C (1998). Detection of chromosomal gains and losses in comparative genomic hybridization analysis based on standard reference intervals. *Cytometry* **31,** 163–173.

[18] ISCN (1995). An International System for Human Cytogenetic Nomenclature Karger Landers, Basel, Switzerland.

[19] Soller MJ, Isaksson M, Elfving P, Soller W, Lundgren R, and Panagopoulos I (2006). Confirmation of the high frequency of the *TMPRSS2/ERG* fusion gene in prostate cancer. *Genes Chromosomes Cancer* **45,** 717–719.

[20] Gleissner B, Rieder H, Thiel E, Fonatsch C, Janssen LA, Heinze B, Janssen JW, Schoch C, Goekbuget N, Maurer J, et al. (2001). Prospective BCR-ABL analysis by polymerase chain reaction (RT-PCR) in adult acute B-lineage lymphoblastic leukemia: reliability of RT–nested-PCR and comparison to cytogenetic data. *Leukemia* **15,** 1834–1840.

[21] Bowman A, Jones D, Medeiros LJ, and Luthra R (2004). Quantitative PCR detection of t(14;18) bcl-2/JH fusion sequences in follicular lymphoma patients: comparison of peripheral blood and bone marrow aspirate samples. *J Mol Diagn* **6,** 396–400.

[22] Haggman MJ, Macoska JA, Wojno KJ, and Oesterling JE (1997). The relationship between prostatic intraepithelial neoplasia and prostate cancer: critical issues. *J Urol* **158,** 12–22.

[23] McNeal JE (1969). Origin and development of carcinoma in the prostate. *Cancer* **23,** 24–34.

[24] McNeal JE and Bostwick DG (1986). Intraductal dysplasia: a premalignant lesion of the prostate. *Hum Pathol* **17,** 64–71.

[25] De Marzo AM, DeWeese TL, Platz EA, Meeker AK, Nakayama M, Epstein JI, Isaacs WB, and Nelson WG (2004). Pathological and molecular mechanisms of prostate carcinogenesis: implications for diagnosis, detection, prevention, and treatment. *J Cell Biochem* **91,** 459–477.